Nephrol Dial Transplant (2015) 30: 434–440
doi: 10.1093/ndt/gfu318
Advance Access publication 16 October 2014

Parathyroid-specific epidermal growth factor-receptor inactivation prevents uremia-induced parathyroid hyperplasia in mice

Maria Vittoria Arcidiacono[1,2,3], Jing Yang[1], Elvira Fernandez[2,3] and Adriana Dusso[1,2,3]

[1]Renal Division, Washington University School of Medicine, St. Louis, MO, USA, [2]Division of Experimental Nephrology, IRB Lleida, Lleida, Spain and [3]Renal Division, Hospital Universitari Arnau de Vilanova, Universidad de Lleida, Lleida, Spain

Correspondence and offprint requests to: Adriana Dusso; E-mail: adusso@irblleida.cat

ORIGINAL ARTICLE

ABSTRACT

Background. In chronic kidney disease (CKD), parathyroid hyperplasia contributes to high serum parathyroid hormone (PTH) and also to an impaired suppression of secondary hyperparathyroidism by calcium, vitamin D and fibroblast growth factor 23 (FGF23). In rats, systemic inhibition of epidermal growth factor receptor (EGFR) activation markedly attenuated uremia-induced parathyroid hyperplasia and vitamin D receptor (VDR) loss, hence restoring the response to vitamin D. Therefore, we propose that parathyroid-specific EGFR inactivation should prevent CKD-induced parathyroid hyperplasia.

Methods. A dominant-negative human EGFR mutant, which forms non-functional heterodimers with full-length endogenous EGFR, was successfully targeted to the parathyroid glands (PTGs) of FVB/N mice, using the 5′ regulatory sequence of the PTH promoter. The parathyroid phenotype and serum chemistries of wild-type (WT) and transgenic mice were examined after 14 weeks of either sham operation or 75% renal mass reduction (NX).

Results. Both genotypes had similar morphology and body weight, and NX-induction enhanced similarly serum blood urea nitrogen compared with sham-operated controls. However, despite similar serum calcium, phosphate and FGF23 levels in NX mice of both genotypes, parathyroid EGFR inactivation sufficed to completely prevent the marked increases in PTG enlargement, serum PTH and in parathyroid levels of transforming growth factor-α, a powerful EGFR-activator, and the VDR reductions observed in WT mice.

Conclusion. In CKD, parathyroid EGFR activation is essential for parathyroid hyperplasia and VDR loss, rendering this transgenic mouse a unique tool to scrutinize the pathogenesis of parathyroid and multiple organ dysfunction of CKD progression unrelated to parathyroid hyperplasia.

Keywords: calcium, phosphate, secondary hyperparathyroidism, transforming growth factor alpha, vitamin D receptor

INTRODUCTION

In chronic kidney disease (CKD), the degree of parathyroid hyperplasia determines the severity of secondary hyperparathyroidism (SHPT) and a poor response to treatment [1, 2]. The increases in parathyroid cell number enhance the capacity of a gland for parathyroid hormone (PTH) synthesis and also reduce parathyroid levels of three critical endogenous regulators of parathyroid cell growth and of PTH synthesis and secretion: the vitamin D receptor (VDR), the calcium sensing receptor (CaSR) and the anti-aging protein α-klotho, a co-receptor of the fibroblast growth factor (FGF) receptor required for fibroblast growth factor 23 (FGF23) actions [2, 3]. Undoubtedly, full delineation of the pathogenesis of parathyroid hyperplasia is essential to improve current strategies for the prevention and treatment of SHPT.

The degree of epidermal growth factor receptor (EGFR) activation is an important molecular link between exacerbated parathyroid cell growth and VDR reductions in rat and human SHPT [4]. In fact, in rat CKD, the three main enhancers of parathyroid cell growth, namely, low calcium, high serum phosphate and vitamin D deficiency induce parathyroid levels of the most potent activator of EGFR-driven growth, transforming growth factor-α (TGFα) [5]. TGFα binding and activation of the EGFR generate a feed-forward cycle for TGFα self-induction and enhanced TGFα/EGFR signals for exacerbated growth and VDR loss. Mechanistically, TGFα/EGFR signals induce the synthesis of a potent oncogene, the dominant-negative isoform of the transcription factor C/EBP β (dnC/EBPβ, also called LIP). Increases in parathyroid LIP not only

exacerbate growth rates but also bind C/EBP sites in the promoter of the VDR gene inhibiting VDR gene expression [4]. Indeed, in a rat model of CKD with high phosphate intake, which reproduces the mild increase in parathyroid gland (PTG) enlargement of human SHPT, systemic halting of EGFR activation with erlotinib, a highly specific EGFR-tyrosine kinase inhibitor, prevented not only further increases in growth rates but also prevented VDR reduction, hence restoring the response to vitamin D in controlling serum PTH [4]. However, erlotinib-control of parathyroid hyperplasia in rat CKD could result, at least in part, from the attenuation of renal damage, as renal TGFα/EGFR signals also mediate glomerulosclerosis, parenchymal lesions including fibrosis, inflammatory infiltration, tubular hyperplasia and proteinuria in mouse [6] and human CKD [7]. Therefore, to delineate the role of EGFR activation on CKD-induced parathyroid hyperplasia *in vivo*, we generated a transgenic mouse with a parathyroid-specific EGFR inactivation, using the dominant-negative strategy shown to successfully inhibit EGFR activation in renal proximal tubular cells [8], and skin keratinocytes [9]. Briefly, most of the cytoplasmic domain of the EGFR containing the tyrosine phosphorylation sites was eliminated to obtain a mutant EGFR (dominant-negative EGFR mutant, dnEGFRm), which acts as a dominant-negative by forming inactive heterodimers with full-length endogenous EGFR.

Herein, the parathyroid phenotype of transgenic and wild-type (WT) littermates was compared after 14 weeks of either the induction of kidney disease by 75% renal mass reduction (NX) or sham operation.

MATERIALS AND METHODS

Plasmid construction and generation of the transgenic mouse

A carboxy-terminally truncated dominant-negative human EGFR mutant, carrying a C-terminus V5 tag and an internal ribosome entry site-green fluorescent protein (IRES-GFP), was targeted to the PTGs using the PTH promoter. First, a carboxy-terminally truncated human EGFR, lacking the last 533 amino acids (EGFRCD533), was subcloned with a C-terminus V5 tag and an IRES-GFP. Specifically, V5 tag and GFP were cloned into the pShuttle vector (Clontech). The EGFRCD533 was polymerase chain reaction amplified with a Kozak sequence and inserted into the modified pShuttle vector. Next, a beta-globin intron was added up to the Kozak-EGFRCD533. Finally, the 5.2 kb Bgl I–Bgl II 5′ regulatory fragment of the human PTH gene, consisting of 5.1 kb of flanking sequence and the first 66 bp or untranslated exon 1 (kindly provided by Dr Arnold, Yale University, Connecticut), was subcloned upstream of the EGFRCD533 to drive the parathyroid-specific expression of the EGFRCD533 mutant, as in [10]. Upon an I-Ceu plus PI-SceI cut, the released fragment containing the human PTH promoter-beta-globin intron-kozak–hEGFRCD533-V5-IRES-GFP-BGHpoly A was prepared for microinjection in FVB/N mice, which develops kidney disease by 2 months after 75% NX.

Fertility was similar in female and male WT and transgenic mice when evaluated at early age (<3 months old) and advanced age (up to 15 months old), as measured by the time for females to get pregnant or for males to fertilize WT females after mating, and also by the size of their litters (average: 5–9 at early age and 6–10 at advanced age).

Parathyroid-specific localization of the transgene

To evaluate the parathyroid expression and sub-cellular location of the transgene in the plasma membrane, as well as its potential non-parathyroid expression, at necropsy, thyroid/parathyroid tissue and non-parathyroid tissues (lung, liver, testis, heart, kidney, spleen and intestine) were embedded in optimal cutting temperature compound media and 5 μm frozen sections were obtained. Standard techniques were used for hematoxylin–eosin staining and V5 (Invitrogen 1:200) immunostaining in frozen sections. GFP expression was examined under a fluorescent microscope.

In situ hybridization for mouse PTH

Dig-RNA antisense and sense probes were obtained from the m-PTH/T-vector, using XhoI to linearize m-PTH/T-vector with T7 polymerase or EcoRI to linearize m-PTH/T-vector, using T3 polymerase. Frozen sections were blocked for 30 min and AP-anti-Dig antibody was added for 60 min. After washing and equilibration, nitro blue tetrazolium/5-bromo-4-chloro-3′-indolyl phosphate color reagent was added and color development was stopped by rinsing with water.

Efficacy of the transgene as a dominant-negative EGFR

Four 75-day-old transgenic mice and four WT littermates were sacrificed 20 min after intra-cardiac injection of EGF (1 μg/g b.w.). Immunostaining for phosphorylated-ERK1/2 (P-ERK; cell signaling 1:25) in thyroid/parathyroid tissue measured the transgene efficacy to reduce EGF activation of endogenous EGFR (Santa Cruz 1:50).

Mouse parathyroid phenotype upon sham operation or 75% NX

Nine-week-old mice underwent the two-step 75% NX procedure described in [8]. Briefly, upon decapsulating the left kidney, upper and lower poles were removed by cauterization to leave half of whole kidney weight. One week later, the right kidney was removed. At necropsy (14 weeks later), blood was collected and frozen sections of thyroid/parathyroid tissue were processed for immunofluorescent analysis of CD45 (Abcam 1:100), TGFα (Calbiochem 1:20), VDR (Millipore 1:50), klotho (R&D Systems 1:100) and PTH (Santa Cruz 1:50) content following standard techniques and using ImageJ software for protein quantification. Cell number per square micrometer was calculated by dividing the number of nuclei visualized by Hoechst staining within the examined parathyroid area. PTH production per cell was obtained by dividing the PTH staining in a PTG area, measured by ImageJ software, by the number of nuclei within the area.

Upon demonstration that three adjacent sections have similar areas (measured by ImageJ software), PTG volume was

estimated by the formula: PTG volume = $\sum$ area (of each measured parathyroid gland section) × height [section thickness = 8 µm × 3 (adjacent sections with similar area)]. The number of 8 µm sections per gland varied from 39 to 85.

For blood chemistries, we used the cresolphthalein-complexone colorimetric assay for plasma calcium, Mouse Intact PTH ELISA Kit (Immutopics) for intact PTH, QuantiChrom™ Urea Assay Kit (Bioassay Systems) for blood urea nitrogen (BUN), QuantiChrome™ Phosphate Assay Kit (DIPI-500, BioAssay System) for plasma phosphate and the mouse FGF-23 Elisa (EMD Millipore) for FGF23.

Statistical analyses

The statistical analysis was performed by a statistician blinded to the experimental conditions using a linear regression model for the mean values of each variable of interest adjusted by both experimental factors (NX and transgene expression) and their interaction (R software). The normality of residuals was checked by the Shapiro–Wilk's normality test. Logarithmic transformation normalized FGF23, PTG size/body weight and parathyroid VDR distributions. Determination coefficients measured goodness of fitness of each model.

RESULTS

Generation of the transgenic mouse

Only one female of the three founders efficiently transmitted the dominant-negative EGFR transgene to its progeny. Indeed, up to F5, there was no difference in parathyroid GFP and V5 expression. The founder's F1 litter showed no difference in the number of WT and transgenic mice, and up to the F5 generation used herein, both mouse genotypes had similar fertility. More significantly, at 2 months of age, WT and transgenic mice with normal kidney function were undistinguishable in size, morphology, body weight and also in skeletal growth, as estimated by tail length [11] either for males and females.

Exclusive parathyroid localization of the dnEGFRm

Figure 1A depicts the analysis of frozen sections of thyroid/parathyroid tissue from 75-day-old WT and transgenic littermates. The V5-tagged dnEGFRm co-localized with GFP protein exclusively in parathyroid tissue, as visualized by *in situ* hybridization for PTH mRNA. There was neither V5 nor GFP expressed in the lung, liver, testis, heart, kidney, spleen or intestine.

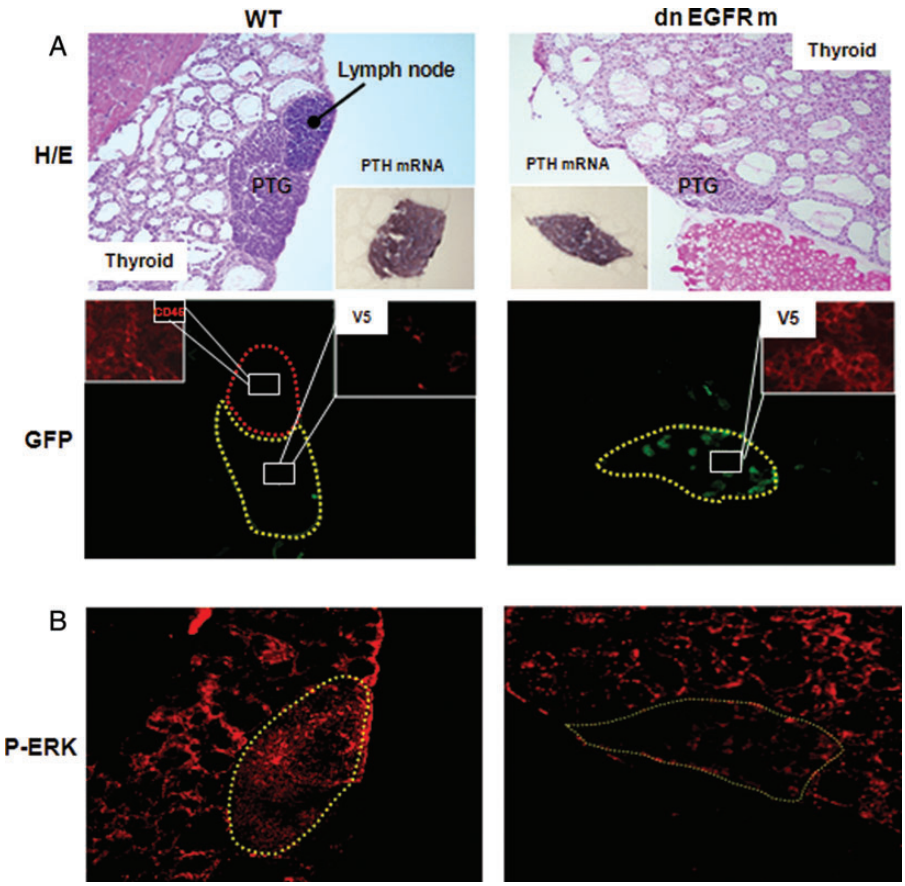

FIGURE 1: Parathyroid-specific localization of a functional dnEGFRm: (**A**, Top) Distinct hematoxylin–eosin (H/E) staining of thyroid and parathyroid tissue and an adjacent lymph node. *In situ* hybridization for PTH mRNA and immunostaining for CD45 (insets) corroborating parathyroid and lymphoid tissue, respectively. (Bottom) Immunofluorescence staining of cells expressing the dnEGFRm tagged with V5 (red) co-localizing with GFP expression (green) exclusively in parathyroid tissue. (**B**) Immunofluorescence staining for P-ERK in thyroid/parathyroid tissue from WT and transgenic mice, in response to EGF injection. Magnification ×100.

The functional efficacy of the transgene as a parathyroid-dominant-negative EGFR was initially examined by comparing EGF activation of endogenous thyroid/parathyroid EGFR in WT and transgenic littermates. Twenty minutes after an intra-cardiac injection of EGF, P-ERK, one-step downstream from EGFR activation, increased similarly in the thyroid tissue of both genotypes. However, P-ERK staining in the PTGs from transgenic mice was markedly lower than in WT littermates (Figure 1B), despite similar levels of endogenous EGFR (WT: 5.99 ± 0.53, $n = 4$; transgenic: 5.60 ± 0.74, $n = 5$). Limitations to locate sufficient PTGs in WT (three of the eight) and transgenic (two of the eight) mice at this young age have impeded the actual assessment of the differences in PTG volume and P-ERK staining. To overcome this limitation and conclusively address the role of a parathyroid-specific EGFR inactivation in CKD-induced parathyroid hyperplasia and VDR loss, we compared the parathyroid phenotype of WT mice and transgenic littermates after 14 weeks of either 75% NX or sham operation.

Parathyroid-specific EGFR inactivation prevented PTG enlargement upon renal mass reduction

Figure 2A shows that by 14 weeks after NX both genotypes elicited similar renal dysfunction. Serum BUN increased similarly in WT mice and their transgenic littermates compared with their respective sham-operated controls. Furthermore, WT and transgenic mice had similar body weight both at the time of NX (WT: 26.5 g ± 0.68, $n = 12$; transgenic: 25.8 ± 1.2, $n = 11$) and 14 weeks after NX (WT: 24.2 ± 0.64, $n = 12$; transgenic: 23.5 ± 0.63; $n = 10$). As expected, serum FGF23 and

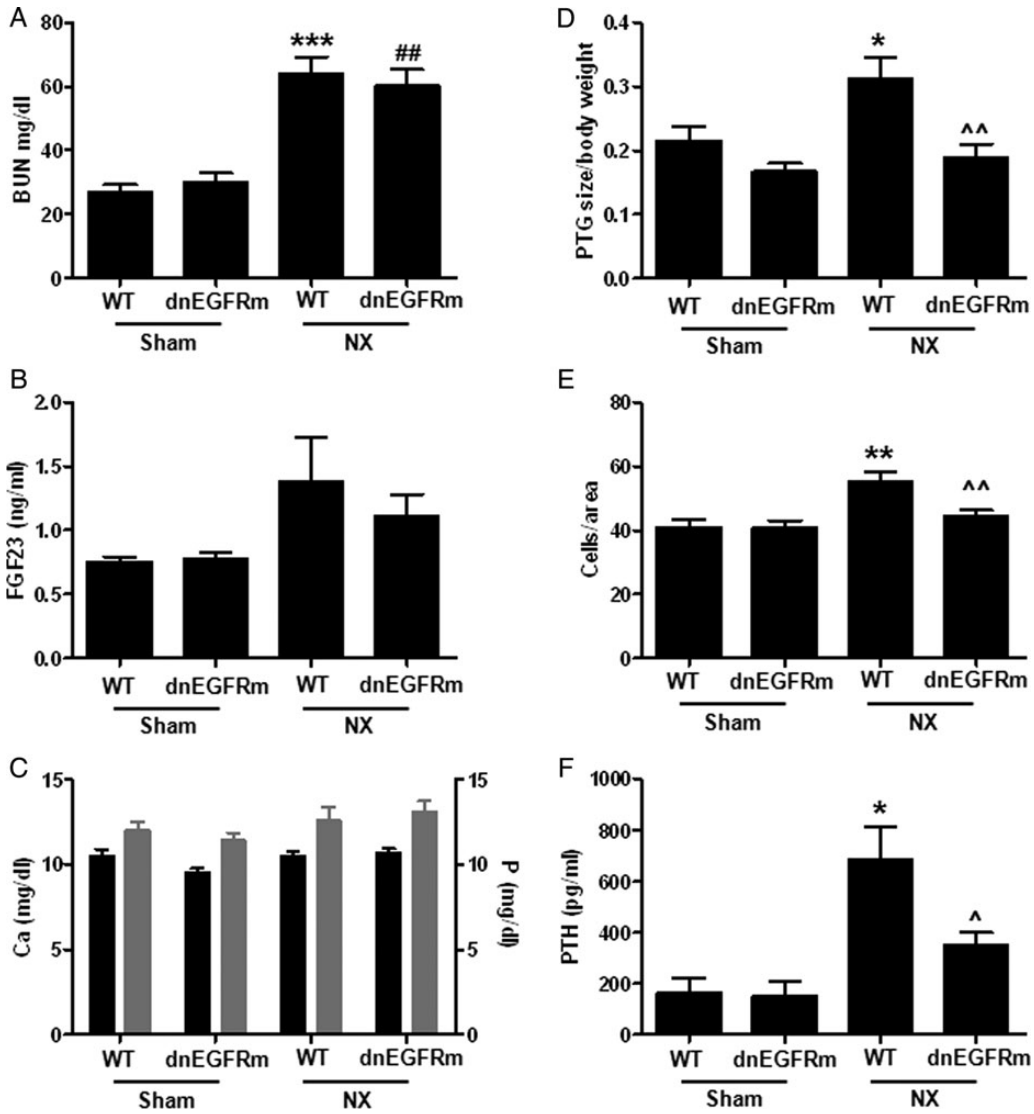

FIGURE 2: Parathyroid-specific EGFR inactivation prevents parathyroid hyperplasia upon NX. Bars and error bars represent the mean and SEM of serum BUN (**A**, $r^2 = 0.50$), FGF23 (**B**, $r^2 = 0.24$) calcium (black bars) and phosphate (gray bars) (**C**, $r^2 = 0.26$ and 0.19, respectively), parathyroid gland volume/body weight (**D**, $r^2 = 0.42$), cell number per PTG area (**E**, $r^2 = 0.62$) and serum PTH (**F**, $r^2 = 0.55$) in WT and dnEGFRm mice after 14 weeks of either 75% NX or sham operation. *, ** or *** indicate $P < 0.05$, $P < 0.01$ or $P < 0.001$ versus sham WT; ## indicates $P < 0.01$ versus sham dnEGFRm; ^ and ^^ indicate $P < 0.05$ and $P < 0.01$ versus NX WT and r^2 measures the goodness of fitness using the linear regression model described in 'Materials and methods' section. No significant interaction between NX and the transgene was found. Sham WT: $n = 5$; sham dnEGFRm: $n = 3$; NX WT: $n = 11$ and NX dnEGFRm: $n = 10$, where n is the number of mice and also the number of parathyroid glands examined.

BUN correlated positively ($r^2 = 0.61$; $n = 12$; $P < 0.04$). Interestingly, despite similar body weight, serum FGF23 (Figure 2B), calcium and phosphate levels (Figure 2C) among experimental groups, only WT mice markedly increased PTG volume (corrected per body weight; Figure 2D), the number of parathyroid cells per area (Figure 2E) and serum PTH (Figure 2F) compared with sham-operated controls. PTH production per cell was similar in NX-WT (0.46 ± 0.13) and NX-transgenic (0.37 ± 0.09, $n = 4$) littermates. In fact, serum PTH correlated significantly with PTG volume ($r = 0.49$; $n = 17$; $P < 0.04$), thus supporting that the lack of increases in parathyroid cell number and PTG enlargement in NX transgenic mice contributed to the maintenance of serum PTH at the levels in normal mice of both genotypes.

Parathyroid-specific EGFR inactivation prevented parathyroid VDR reductions upon renal mass reduction

Parathyroid expression of the dnEGFRm prevented the 3-fold enhancement in parathyroid TGFα levels induced by NX in WT mice ($P < 0.001$; Figure 3A and B, left panels) supporting the efficacy of the transgene to inhibit TGFα activation of endogenous EGFR self-induction.

Furthermore, parathyroid-specific EGFR inactivation prevented CKD-induced reductions in parathyroid cytosolic and nuclear VDR seen in WT mice (Figure 3A and B, right panels). Indeed, in transgenic mice, the parathyroid VDR content after 14 weeks of uremia was similar to that in sham-operated controls. These effects of the transgene appear to be VDR specific, as parathyroid klotho staining was similar in WT mice (IOD/area WT: 51.1 ± 4.3, $n = 3$) and transgenic (57.3 ± 7.4 $n = 4$) littermates.

DISCUSSION

This work presents the successful generation of a transgenic mouse harboring a parathyroid-specific EGFR inactivation, whose parathyroid phenotype has conclusively demonstrated the essential role of parathyroid EGFR activation in the CKD-induced development of parathyroid hyperplasia, TGFα self-induction and consequently in high serum PTH as well as in the VDR reductions responsible for the poor response to vitamin D therapy. The translational relevance of this mouse model in nephrology is high, as it provides a unique tool to scrutinize *in vivo* targetable mechanisms underlying CKD-induced abnormalities in PTH synthesis and secretion and in the response to therapy that are unrelated to the degree of parathyroid hyperplasia or VDR reduction.

In a low cell turnover tissue as the PTG [12, 13], proliferation rates increase only when more cells are needed to meet

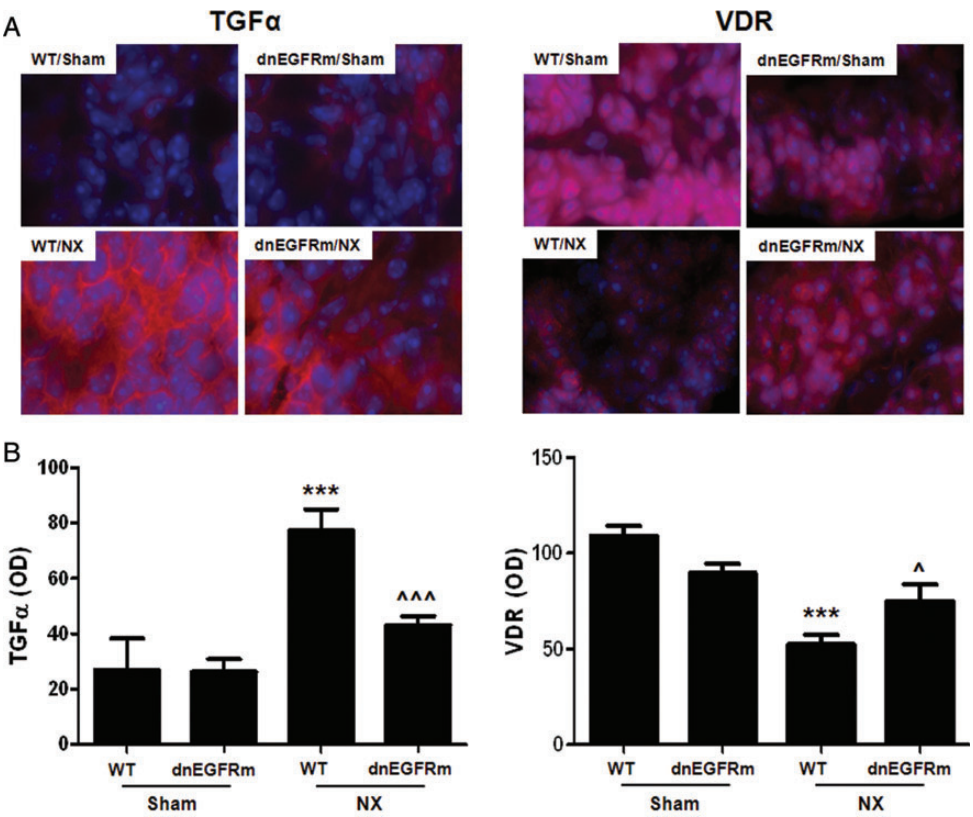

FIGURE 3: Parathyroid-specific EGFR inactivation attenuates the increases in parathyroid TGFα and prevents VDR reductions upon NX. (**A**) Representative immunofluorescence staining of parathyroid TGFα (left) and VDR (right) content (red, AlexaFluor 594) and nuclei (blue, Hoechst). (**B**) Bars and error bars represent the mean and SEM parathyroid TGFα (left) or VDR (right) staining in WT and dnEGFRm mice after 14 weeks of either 75% NX or sham operation. *** indicates $P < 0.001$ versus sham WT; ^, ^^^ indicate $P < 0.05$, $P < 0.001$ versus NX WT; r^2 of 0.74 for TGFα and 0.56 for VDR indicate the goodness of fitness of the linear regression model described in 'Materials and methods' section. There was also a significant interaction between NX and transgene expression of $P < 0.03$ and $P < 0.04$, respectively.

the requirements for higher serum PTH triggered by an initial stimulus [14]. Indeed, high P, low Ca and vitamin D deficiency are recognized stimuli for PTH hypersecretion and parathyroid cell growth in health, and also markedly aggravate the elevations in serum PTH and growth rates induced by CKD [2]. In contrast, the response of the PTG to increases in FGF23, which suppress PTH secretion and cell growth in normal glands, fails in CKD [2] due to reductions in parathyroid klotho and FGFR1 [15–17], causing defective klotho-dependent and FGFR-dependent/klotho-independent FGF23 signaling [18].

A role for EGFR activation in the severity of parathyroid hyperplasia was initially suggested by the enhanced parathyroid TGFα levels, the most potent EGFR-activating ligand, in adenomas and in hyperplastic PTGs from primary hyperparathyroidism and CKD patients [19]. Also in rat CKD, marked increases in parathyroid TGFα in response to high P or low Ca diets caused the doubling of PTG size within 1 week after 5/6 NX [5]. Furthermore, in rat CKD, systemic administration of highly specific inhibitors of EGFR activation prevented high P- or low Ca-induced PTG enlargement with an efficacy comparable to that of high Ca intake, P restriction or prophylactic administration of active vitamin D [5]. Similarly, using a rat model of established SHPT and high P intake for a month, which mimics the slower progression of parathyroid hyperplasia of human CKD, administration of highly specific EGFR inhibitors was sufficient to prevent further enhancement of parathyroid TGFα, PTG enlargement and VDR reductions, with an efficacy comparable to that of phosphate restriction [4]. However, systemic inhibition of EGFR activation could also suppress renal TGFα/EGFR signals that compromise kidney function [6, 8], which could in turn help maintain renal response to the increased FGF23 in inducing phosphaturia, thereby attenuating high phosphate induction of parathyroid cell growth and PTH secretion [2, 15]. Therefore, although it was expected that the successful expression of a parathyroid dnEGFRm could attenuate CKD-induced PTG enlargement and the increases in parathyroid TGFα resulting in lower serum PTH levels, the observed complete prevention of PTG enlargement and elevations in serum PTH was quite striking. The efficacy of the transgene in preventing parathyroid TGFα/EGFR signals driving aggressive growth, including TGFα induction of its own expression, is of high clinical relevance. In rat and human hyperparathyroidism, the levels of parathyroid TGFα correlated not only with the number of parathyroid cells staining positive for the marker of cell proliferation, PCNA, but also with activator protein-2, an inducer of TGFα gene transcription [20]. Herein, the higher number of parathyroid cells per area in enlarged PTGs occurred exclusively in WT uremic mice, thus corroborating in mouse CKD that the higher proliferating rates result from enhanced EGFR activation by the increased parathyroid TGFα. Undoubtedly, this finding also demonstrates that there is little, if any, role for impaired response to high FGF23/FGFR-signaling, both klotho-dependent [15–17] and the novel klotho-independent signals involving a calcineurin-dependent pathway [18], in CKD-induced parathyroid hyperplasia in mice, at least at this early CKD stage.

Equally relevant for therapy was our demonstration that preventing parathyroid EGFR activation sufficed to maintain in NX mice the parathyroid VDR content of sham-operated controls. Surprisingly, the transgene had no influence on parathyroid klotho despite its efficacy in preventing both hyperplasia and reductions in VDR, a transcriptional inducer of the klotho gene [21]. This finding unraveled an abnormal regulation of parathyroid klotho expression in uremia unrelated to either hyperplastic growth or VDR loss. Although the impact of the transgene on parathyroid levels of the CaSR and FGFR could not be measured, similar to the VDR or klotho, it is their activity rather than their actual expression, which is critical to efficaciously suppress PTH synthesis and secretion. Thus, this transgenic mouse provides a unique and important tool to identify optimal interventions with vitamin D, calcimimetic or anti-calcineurin drugs to correct *in vivo* CKD-mediated abnormalities in PTH synthesis and secretion in the absence of hyperplasia or VDR loss. In addition, this model can help identify the time point during CKD progression, at which normal serum PTH will be insufficient to maintain normal Ca and P.

The similar PTGs size in normal mice of both genotypes suggests that EGFR activation is not necessary for normal PTG growth. Intriguingly, TGFα activation of the EGFR is essential for embryonic PTG development [22]. Indeed, the ADAM17 null mice, lacking the enzyme that releases mature TGFα for EGFR activation, die perinatally due to severe defects in the morphogenesis of numerous epithelial organs including the PTGs [22]. Therefore, it is possible that a marginal EGFR activation in the transgenic mice is sufficient to support the slow rate of embryonic (doubling times of 7–10 days) and postnatal PTG growth [12–14]. Alternatively, an embryonic compensation to the endogenous EGFR inactivation imposed by the dnEGFRm might have occurred to ensure normal mineral and skeletal homeostasis, at least up to 5 months of age.

In summary, this transgenic model underscores the importance of preventing EGFR activation to effectively suppress the development of parathyroid hyperplasia and VDR loss in early CKD and provides a unique tool to identify both novel targetable regulators of abnormal PTH synthesis and secretion in CKD unrelated to parathyroid hyperplasia or VDR loss, and CKD-induced abnormalities in bone remodeling and multiple organ dysfunction that are unrelated to the degree of SHPT.

ACKNOWLEDGEMENTS

The authors thank Montserrat Martinez-Alonso (Department of Statistics, IRB Lleida) for her valuable assistance in conducting the Statistical Analysis. This work was supported by the following grants to A.D.: RO1 DK062713 from NIDDK; CEDAR (Center for D-receptor Activation Research); Abbott Pharmaceuticals, FIS PI11/00259 from Institutos de Salud Carlos III, Spanish Government and the Barnes Jewish Auxiliary Chapter. The generation of the transgenic mouse at the experimental genetic core facility at Washington University, and the processing for serum chemistries were partly supported by Core C of the O'Brien Center for renal chemistries, Grant P30DK079333.

CONFLICT OF INTEREST STATEMENT

None declared.

REFERENCES

1. Kidney Disease: Improving Global Outcomes CKD-MBD Work Group. KDIGO clinical practice guideline for the diagnosis, evaluation, prevention, and treatment of Chronic Kidney Disease-Mineral and Bone Disorder (CKD-MBD). Kidney Int Suppl 2009; 113: S1–130
2. Silver J, Rodriguez M, Slatopolsky E. FGF23 and PTH—double agents at the heart of CKD. Nephrol Dial Transplant 2012; 27: 1715–1720
3. Silver J, Naveh-Many T. FGF-23 and secondary hyperparathyroidism in chronic kidney disease. Nat Rev Nephrol 2013; 9: 641–649
4. Arcidiacono MV, Sato T, Alvarez-Hernandez D *et al.* EGFR activation increases parathyroid hyperplasia and calcitriol resistance in kidney disease. J Am Soc Nephrol 2008; 19: 310–320
5. Cozzolino M, Lu Y, Sato T *et al.* A critical role for enhanced TGF-alpha and EGFR expression in the initiation of parathyroid hyperplasia in experimental kidney disease. Am J Physiol Renal Physiol 2005; 289: F1096–F1102
6. Lautrette A, Li S, Alili R *et al.* Angiotensin II and EGF receptor cross-talk in chronic kidney diseases: a new therapeutic approach. Nat Med 2005; 11: 867–874
7. Melenhorst WB, Visser L, Timmer A *et al.* ADAM17 upregulation in human renal disease: a role in modulating TGF-alpha availability? Am J Physiol Renal Physiol 2009; 297: F781–F790
8. Terzi F, Burtin M, Hekmati M *et al.* Targeted expression of a dominant-negative EGF-R in the kidney reduces tubulo-interstitial lesions after renal injury. J Clin Invest 2000; 106: 225–234
9. Murillas R, Larcher F, Conti CJ *et al.* Expression of a dominant negative mutant of epidermal growth factor receptor in the epidermis of transgenic mice elicits striking alterations in hair follicle development and skin structure. EMBO J 1995; 14: 5216–5223
10. Imanishi Y, Hosokawa Y, Yoshimoto K *et al.* Primary hyperparathyroidism caused by parathyroid-targeted overexpression of cyclin D1 in transgenic mice. J Clin Invest 2001; 107: 1093–1102
11. Schrick JJ, Dickinson ME, Hogan BL *et al.* Molecular and phenotypic characterization of a new mouse insertional mutation that causes a defect in the distal vertebrae of the spine. Genetics 1995; 140: 1061–1067
12. Wang Q, Palnitkar S, Parfitt AM. Parathyroid cell proliferation in the rat: effect of age and of phosphate administration and recovery. Endocrinology 1996; 137: 4558–4562
13. Wang Q, Palnitkar S, Parfitt AM. The basal rate of cell proliferation in normal human parathyroid tissue: implications for the pathogenesis of hyperparathyroidism. Clin Endocrinol (Oxf) 1997; 46: 343–349
14. Parfitt AM. The hyperparathyroidism of chronic renal failure: a disorder of growth. Kidney Int 1997; 52: 3–9
15. Komaba H, Goto S, Fujii H *et al.* Depressed expression of Klotho and FGF receptor 1 in hyperplastic parathyroid glands from uremic patients. Kidney Int 2010; 77: 232–238
16. Galitzer H, Ben-Dov IZ, Silver J *et al.* Parathyroid cell resistance to fibroblast growth factor 23 in secondary hyperparathyroidism of chronic kidney disease. Kidney Int 2010; 77: 211–218
17. Canalejo R, Canalejo A, Martinez-Moreno JM *et al.* FGF23 fails to inhibit uremic parathyroid glands. J Am Soc Nephrol 2010; 21: 1125–1135
18. Olauson H, Lindberg K, Amin R *et al.* Parathyroid-specific deletion of Klotho unravels a novel calcineurin-dependent FGF23 signaling pathway that regulates PTH secretion. PLoS Genet 2013; 9: e1003975
19. Gogusev J, Duchambon P, Stoermann-Chopard C *et al.* De novo expression of transforming growth factor-alpha in parathyroid gland tissue of patients with primary or secondary uraemic hyperparathyroidism. Nephrol Dial Transplant 1996; 11: 2155–2162
20. Arcidiacono MV, Cozzolino M, Spiegel N *et al.* Activator protein 2alpha mediates parathyroid TGF-alpha self-induction in secondary hyperparathyroidism. J Am Soc Nephrol 2008; 19: 1919–1928
21. Forster RE, Jurutka PW, Hsieh JC *et al.* Vitamin D receptor controls expression of the anti-aging klotho gene in mouse and human renal cells. Biochem Biophys Res Commun 2011; 414: 557–562
22. Peschon JJ, Slack JL, Reddy P *et al.* An essential role for ectodomain shedding in mammalian development. Science 1998; 282: 1281–1284

Received for publication: 17.4.2014; Accepted in revised form: 5.9.2014